DESIGN AND ANALYSIS OF A THREE-PHASE THREE-STACK CLAW POLE PERMANENT MAGNET MOTOR WITH SMC STATOR

Y.G. Guo*, J.G. Zhu*, P.A. Watterson*, and W. Wu**

*Faculty of Engineering, University of Technology, Sydney, P.O. Box 123, Broadway, NSW 2007, Australia

**CSIRO Telecommunications and Industrial Physics, P.O. Box 218, Lindfield, NSW 2070, Australia

Abstract

This paper reports the design, performance analysis, and prototype experiment of a three-phase three-stack permanent magnet claw pole motor with a soft magnetic composite stator. To predict and optimise the major parameters and motor characteristics, a three-dimensional finite element analysis of magnetic field is performed. The parameter calculation and performance analyses are validated by experiment on a prototype.

1. INTRODUCTION

Soft magnetic composite (SMC) materials produced by powder metallurgy techniques have undergone significant development in the past few years because of their unique properties and potential application in electrical machines [1,2]. This type of material is made of iron powder of high purity and compressibility. The grains are bonded with a coating of an organic material, which produces high electrical resistivity. The coated powder is then pressed into solid material using a die and finally heat treated to anneal and cure the bond.

Compared with electrical steels widely used in rotating machines and transformers, the major advantage of the SMC material is the prospect of large volume manufacturing of low cost electromagnetic devices. Because the iron cores and parts can be pressed in a die into the desired shape and dimension, the further machining is minimised and hence the production cost is greatly reduced. In addition, the powdered nature of the material yields lower eddy current losses and isotropic magnetic properties. Therefore, it is suitable for specially structured, such as claw pole, motors with three-dimensional (3D) fluxes. The permeability of this material, however, is lower than that of electrical steels. It is expected that this material would be appropriate for construction of permanent magnet (PM) motors for which the magnetic reluctance of the magnet dominates the magnetic circuit, making such motors less sensitive to the permeability of the core than armature magnetised machines, e.g. induction and reluctance machines.

This paper presents the design, performance analysis, prototype construction, and experiment of a 3-phase 3-stack PM claw pole motor with an SMC stator. SOMALOY™ 500, a new soft magnetic composite produced by Höganäs AB, Sweden, is used as the stator core material. It is characterised by a thin continuous surface insulation layer with little or no effect on the powder compressibility.

The major motor parameters are calculated based on the magnetic field distribution through 3D finite element method (FEM). Rotational core losses of SOMALOY™ 500 with rotating magnetic fluxes at different frequencies were measured using a single sheet rotational core loss tester [3] and applied in the performance calculation.

2. STRUCTURE AND DIMENSIONS

Due to the nearly universal use in automobile alternators, electrical machines with claw pole rotors have been manufactured in mass production for many years. These machines have quite simple excitation coil and pole systems producing the excitation magnetic fields. They are capable of producing power densities up to three times greater than the conventional machines because their topology allows the pole number to be increased without reducing the magnetomotive force per pole. The excessive eddy currents in the commonly used solid steel core, however, limit the motors to very small sizes and/or low speeds and results in low efficiency.

Because of the complex structure, it is very difficult to construct the claw poles using lamination steels. SMC offers an opportunity to overcome these problems.

Fig. 1 illustrates the magnetically relevant parts of the rotor and the stator of the prototype. Table 1 lists the dimensions and major parameters. The three phases of the motor are stacked axially. Each stator phase has a single coil around an SMC core, which is molded in two halves. The outer rotor comprises a tube of mild steel with an array of magnets for each phase mounted on the inner surface. Mild steel is used for the rotor because the flux density in the yoke is almost constant.

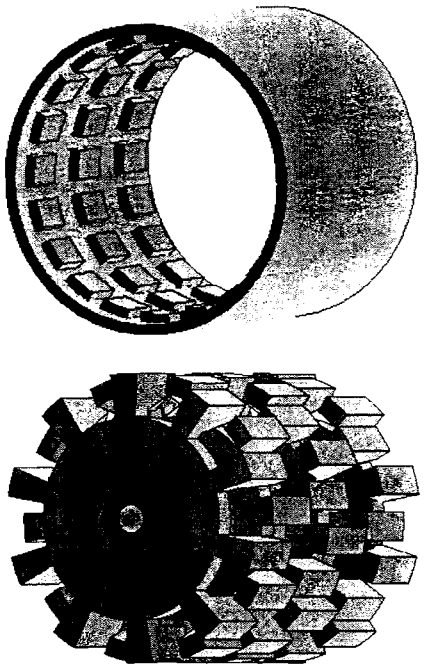

Fig. 1 Magnetically relevant parts of the claw pole motor

Table 1: Dimensions and major parameters

Dimensions and parameters	Quantities
Rated frequency (Hz)	300
Number of phases	3
Rated power (W)	500
Rated line-to-neutral voltage (V)	64
Rated phase current (A)	4
Rated speed (rev/min)	1800
Rated torque (Nm)	2.65
Rated efficiency (%)	85
Rated temperature rise (°C)	75
Number of poles	20
Stator core material	SOMALOY™ 500
Stator outer radius (mm)	40
Effective stator axial length (mm)	93
Rotor outer radius (mm)	48
Rotor inner radius (mm)	41
Permanent magnets	NdFeB, Grade N30M
Number of magnets	60
Magnet dimensions	OD88 x ID82 x 15 mm arc 12°
Magnetization directions	Radially outward and inward
Main airgap length (mm)	1
Sub-airgap length* (mm)	4.2
Stator shaft material	Mild steel
Shaft outer radius (mm)	9
Number of coils	3
Coil window dimension (mm^2)	17 x 11
Number of turns	75
Number of strands	2
Diameter of copper wire (mm)	0.71
Resistance per phase at 115°C (Ω)	0.302

* The sub-airgap is defined as the gap between the sides of the claw poles of the two separated pieces.

For the prototype, the motor size and core geometry were to a large extent determined by the dimensions of the available SOMALOY™ 500 preforms. They were chosen the same as those of a PM SMC transverse flux motor prototype, enabling comparison [4]. A pole number of 20 was chosen giving an operating frequency of 300 Hz at 1800 rpm. It is not an unrealistically high frequency to work at for SMC materials. Since a simple concentrated stator winding is used, a reasonably high fill factor can be achieved and the manufacturing cost can be very low.

3. 3D MAGNETIC FIELD ANALYSIS

The magnetic circuits of three stacks (or phases) of the motor are basically independent. For each stack, because of the symmetrical structure, it is only required to analyse the magnetic field in one pole pitch, as shown in Fig. 2.

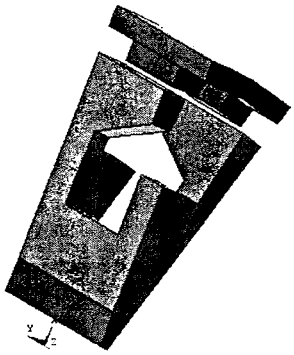

Fig. 2 Region for field solution

At the two radial boundary planes of one pole pitch, the magnetic scalar potential obeys the so-called half-periodical boundary conditions:

$$\varphi_m(r, \Delta\theta/2, z) = -\varphi_m(r, -\Delta\theta/2, -z) \quad (1)$$

where $\Delta\theta = 18°$ is the angle of one pole pitch. The original point of the cylindrical coordinate is located at the centre of the stack.

3.1 Magnetic Flux Linking the Stator Winding at No-load

As the rotor rotates, the flux linking the stator winding varies and an electromotive force (*EMF*) is induced. The *EMF* frequency depends on the rotor speed, while its waveform is determined by the waveform of the flux. At no-load, the flux waveform was calculated by rotating the rotor for one pole pitch in 12 steps. As plotted in Fig. 3, this flux waveform versus the rotor position is almost perfectly sinusoidal. In the design, the motor structure and dimensions have been adjusted such that the peak flux linkage of the stator winding is the maximum.

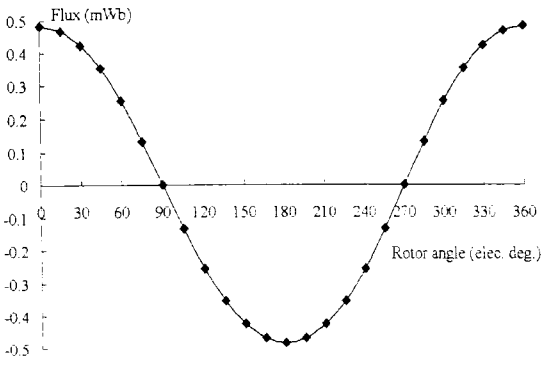

Fig. 3 No-load flux per turn of a phase winding

3.2 Cogging Torque

Cogging torque is caused by the tendency of the rotor to line up with the stator in a particular direction where the magnetic circuit has the highest permeance. The cogging torque arises from the reluctance variation of the magnetic circuit as the rotor rotates and exists even when there is no stator current. Fig. 4 shows the cogging torque versus the rotor position for one phase of the machine, calculated by the Coulomb virtual work method. This curve was calculated by rotating the rotor for one pole pitch in 12 steps, i.e. 1.5° (mechanical) per step.

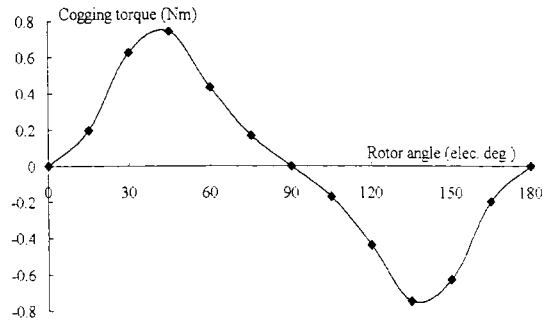

Fig. 4 Cogging torque versus rotor position for one stack

The cogging torque has a period of 180 electrical degrees and anti-symmetry about zero, hence only even sine harmonics, which were computed by the Discrete Fourier Transformation (DFT) method to be

$$T_A \approx 0.6150\sin 2\theta + 0.0629\sin 4\theta - 0.1270\sin 6\theta - 0.0479\sin 8\theta + 0.0030\sin 10\theta + 0.0001\sin 12\theta \quad (2)$$

where θ is the rotor angle in electrical degrees. The stator claw pole teeth on the three phases are shifted by 120 electrical degrees, and all even harmonics other than order 6 or its multiples sum to zero over the three phases. The magnitudes of the 6^{th} and 12^{th} harmonics of cogging torque are 0.3810 Nm and 0.0003 Nm, respectively.

3.3 Inductance and Armature Reaction

The self- inductance of each phase winding can be calculated by

$$L_1 = \frac{N_1\phi_1}{I_1} \quad (3)$$

where ϕ_1 is the magnitude of the flux linking the stator winding due to a stator current I_1 in each of N_1 turns. It can be obtained from the results of a field analysis with a stator current I_1 while the permanent magnets are "switched off", i.e. remanence is set to zero. In this three-phase motor, the mutual inductance between phase windings can be considered as zero since the magnetic circuit for each phase is basically independent. From Table 2, it can be seen that the per-turn inductance is very uniform against rotor angles. The inductance scales as N_1^2 and so is 5.24 mH for 75 turns. It is also shown in Table 2 that the armature reaction for rated current is quite small and it will not demagnetise the magnets.

Table 2: Inductance and armature reaction in magnets

Rotor position (elec. deg.)	Self inductance per turn (μH)	Maximum B in magnets (T)
0	0.932	0.031
45	0.932	0.030
90	0.932	0.037

3.4 Core Loss Calculation

The core loss is caused not only by alternating but also by rotational magnetic fields, and should be considered properly in the design [5]. The **B-H** relationship and specific core losses of SMC material SOMALOY™ 500 used for the stator core were measured under a 2D rotating excitation [3]. The quasi-3D properties were also obtained by the 2D tests and applied in the design calculation.

In claw pole machines, the armature carries significant fluxes in all directions. An improved method is applied for predicting core losses of 3D-flux SMC machines in [6]. Different formulations are used for core loss prediction with purely alternating, purely circular rotating, and elliptically rotating flux density vectors, respectively. A series of 3D finite element analyses are conducted to determine the flux density locus in each element when the rotor rotates. The calculated no load core loss, varied approximately linearly with frequency and was 58.0 W at 300 Hz. Under rated load it will increase by about 20%.

3.5 Optimisation of Magnet Length

Taking advantage of the isotropic magnetic property of SMC material, the magnet length can be chosen

longer than the claw pole to obtain higher stator flux and hence higher specific torque. However, too much magnet overhang may lead to saturation and is cost-ineffective. Comparing the ratio of torque to overall material cost, the magnet length is chosen as 15 mm, which exceeds the claw pole head by 1.65 mm.

3.6 Flux Penetration in Stator Shaft

In the field analysis, the flux is assumed not to pass through the stator shaft since the mild steel shaft has much higher conductivity and permeability than the SMC yoke, as shown in Table 3.

Table 3: Comparison of SMC and mild steel

Parameters	SMC	Mild steel
Relative permeability	130	5000 (range 1500 –10000)
Conductivity (S/m)	500 - 10000	1.12×10^7
Penetration or skin depth at 300 Hz (mm)	25.5 – 114	0.123

The penetration or skin depth can be calculated by

$$\delta = \sqrt{\frac{2}{\omega\mu\sigma}} \tag{4}$$

where μ is the magnetic permeability of the material, σ the electrical conductivity, and ω the angular frequency of the flux. Assuming linear permeability, the flux penetrating the shaft and the eddy current loss are given by [7],

$$\phi = B_p(2\pi r_{shaft})\frac{\delta}{\sqrt{2}} \tag{5}$$

$$w_e = \frac{B_p^{\,2}}{2\mu^2\sigma\delta}(2\pi r_{shaft} l_{shaft}) \tag{6}$$

where B_P is the peak flux density just inside the shaft surface, r_{shaft} is the shaft radius, and l_{shaft} is the effective shaft length. The maximum flux density in the stator yoke is about 1.0 T, kept low to reduce core loss. By continuity of tangential magnetic field strength, B_P will be saturated, around 2 T. Though Eq. (5) and Eq. (6) are for non-saturated material, if applied they give that the penetrating flux and eddy current loss in the mild steel shaft at 300 Hz are only 0.007 mWb and 0.096 W, respectively. Compared to the flux and core loss in the SMC yoke, these values are negligible.

3.7 Eddy Current in SMC

Since it is very difficult to model the complex cyclic magnetization of SMC in the FEM magnetic field analysis, a single valued B-H curve is used instead and iron loss is then estimated as a post-processor exercise. This approach may have a risk in calculating eddy current [2]. The insulation between grains in SMC is not perfect and significant bulk eddy current, which flows between grains, may well be present. The ratio of the material dimensions to skin depth is a critical parameter. If the smallest dimension of the component normal to the magnetic field plane is near the skin depth the field will be significantly disturbed by the eddy currents and will be restricted to near the surface of the component. The result is that the effective permeability falls, a phase shift is introduced, high loss is induced, and the skin effect must be part of the analysis, which is far more complex.

The narrowest dimensions for the SMC claw pole teeth, claw pole discs, and the stator yoke are 5 mm, 7 mm and 10 mm, respectively. They are much lower than the skin depth at the rated frequency, as in Table 3. Thus, the magnetic field analysis can be conducted ignoring eddy currents.

3.8 Thermal Analysis

To obtain an economic utilisation of the materials and safe operation of the motor it is necessary to predict with reasonable accuracy the temperature rise of the internal parts, especially in the coils and magnets. In this paper, the temperature rise is calculated by using an equivalent thermal circuit as shown in Fig. 5. The copper loss P_{cu}, core loss P_{Fe}, and mechanical loss P_{mec} are the thermal sources.

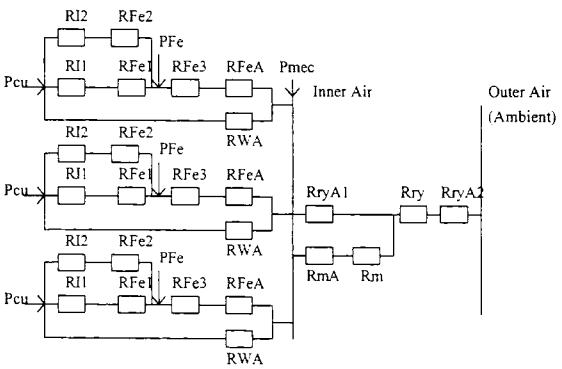

Fig. 5 Equivalent thermal circuit

4. PERFORMANCE CALCULATION

The motor uses a standard six-transistor bridge drive circuit. With open-loop control, the motor can operate in normal synchronous mode. With the closed-loop control of position feedback it can also operate in brushless DC mode where the current I_1 and the induced *EMF*, E_1 in the stator winding are in phase, to achieve a maximum electromagnetic power P_{em} at a given speed, i.e.

$$P_{em} = 3E_1 I_1 \tag{7}$$

The induced stator *EMF* can be determined by

$$E_1 = \frac{\omega_1 N_1 \phi_m}{\sqrt{2}} \tag{8}$$

where $\omega_1=2\pi f_1$ is the angular rotor speed in electrical radians per second, f_1 the frequency of the induced stator *EMF* in Hertz, N_1 the number of turns of the stator winding, and ϕ_m the magnitude of the magnetic flux linking the stator winding due to the permanent magnets.

The rated line-to-neutral rms voltage by:

$$V_1 = \sqrt{(E_1 + I_1 R_1)^2 + (I_1 X_1)^2} \tag{9}$$

where R_1 is the resistance of one phase winding and X_1 is the reactance. At 1800 rpm (300Hz), E_1= 48.7 V, and for a rated current of 4 A, limited by the temperature rise of the stator winding, P_{em}=585 W and V_1=63.7 V. The corresponding DC input voltage of the inverter can be estimated by

$$V_{dc} = 2.34 V_1 \tag{10}$$

The output power, output torque, input power, and efficiency are calculated by

$$P_{out} = P_{em} - P_{Fe} - P_{mec} \tag{11}$$

$$T_{out} = P_{out} / \omega_r \tag{12}$$

$$P_{in} = P_{em} + P_{cu} \tag{13}$$

$$P_{cu} = 3 I_1^2 R_1 \tag{14}$$

$$\eta = P_{out} / P_{in} \tag{15}$$

where P_{Fe} is the core loss, P_{mec} the mechanical loss, P_{cu} the copper loss, and ω_r is the angular speed. At the rated operation, the efficiency is calculated as 85%.

At a given voltage input, the steady state characteristic with optimum feedback can be predicted by

$$\omega_r = \frac{V_1}{K_e} - \frac{R_1}{K_e K_T} T_{em} \tag{16}$$

where K_e is the back *EMF* constant, K_T the torque constant, and T_{em} is the electromagnetic torque.

5. EXPERIMENT VALIDATION

Fig. 6 shows the setup of the 3-phase 3-stack claw pole PM motor with SMC stator core (on the right). A DC machine (on the left) is connected via a torque transducer (in the middle) as the load when the prototype operates as a motor, or the driver when the prototype operates as a generator.

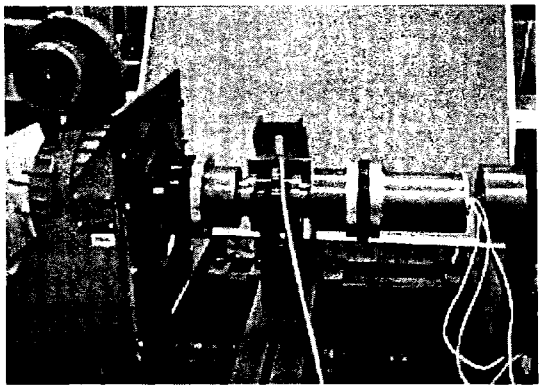

Fig. 6 Test set-up of a claw pole PM motor with SMC stator

5.1 Measurement of Resistance and Inductance

When a DC current I_{dc} of 1 A is fed through the stator winding, the voltage V_{dc} across the winding is measured and then the resistance can be calculated by

$$R_1 = V_{dc} / I_{dc} \tag{17}$$

When an AC voltage V_{ac} with frequency f_1 is applied across the stator winding, the current flowing through the winding I_{ac} is measured and then the inductance can be calculated by

$$L_1 = \frac{\sqrt{(V_{ac} / I_{ac})^2 - R_1^2}}{2\pi f_1} \tag{18}$$

The measured phase resistance is 0.225 Ω at room temperature or 0.3 Ω at 115 °C, and the measured phase inductance is 5.79 mH. They are in a good agreement with the prediction.

5.2 Temperature Rise

The copper temperature is measured by the resistance method, comparing the resistance R_1 at room temperature t_1 and the measured resistance R_2 immediately after the load test. Since the thermal time constant is quite large, the copper temperature will not drop very quickly.

$$t_2 = \frac{R_2}{R_1}(234.5 + t_1) - 234.5 \ ^\circ\mathrm{C} \tag{19}$$

The temperature measured by this method is the average of the winding. A factor needs to be added for the hottest spot. To detect the rotor yoke temperature, an infrared temperature probe is used.

5.3 Back EMF Waveform

When the prototype operates as a generator, driven by the DC machine, the back electromotive force can be measured from the open circuit voltage. Fig. 7 shows the measured *EMF* waveforms, which are very close to sinusoidal. The waveforms of three phases are with the same magnitude but shifted each other by 120 electrical degrees in phase angles.

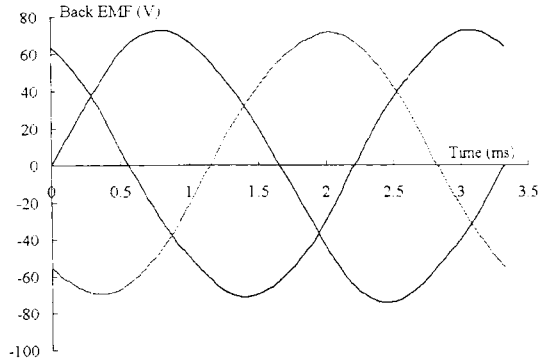

Fig. 7 Measured back EMF waveforms at 1800 rpm

5.4 Steady State Characteristics

The steady state characteristics were measured by using a DC/AC inverter and a sensorless controller. The parameters of the controller were adjusted to obtain the optimum performance. Fig. 8 shows the speed versus torque for different inverter DC voltages.

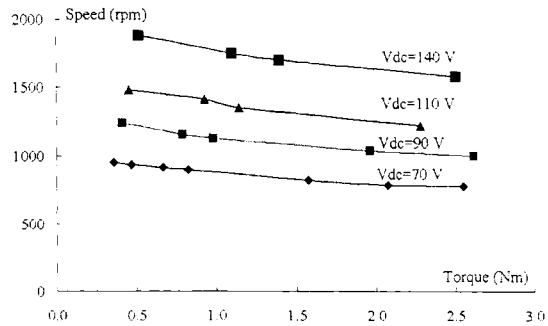

Fig. 8 Speed versus torque with different input DC voltages

5.5 Core Loss and Efficiency

The core loss was measured by the dummy stator method, detailed in [6]. The efficiency at the rated operation condition was measured as 84%, in a good agreement with the calculation.

6. CONCLUSION AND DISCUSSION

To investigate the potential of SMC materials in manufacturing of small motors of complex structures, a 3-phase PM claw pole motor with SMC core has been designed and manufactured. The prototype performance is comparable to that of similar motors with electrical steel cores at potentially reduced manufacturing cost. The method for the motor design and performance analysis has been validated by the experiment on the motor.

7. ACKNOWLEDGEMENT

The authors wish to thank Höganäs AB, Sweden, for supplying preforms of SOMALOY™ 500.

8. REFERENCES

[1] "The Latest Development in Soft Magnetic Composite Technology from Höganäs Metal Powders", *Höganäs Manual – SMC Update, www.hoganas.com*, 1997-2003

[2] Jansson, P. and Jack, A.G., "Magnetic Assessment of SMC Materials", *Twenty First Annual Conference on Properties and Applications of Magnetic Materials*, Chicago, USA, May 2002, pp 1-9

[3] Zhu, J.G, Zhong, J.J., Ramsden, V.S., and Guo, Y.G., "Power Losses of Composite Soft Magnetic Materials under Two Dimensional Excitations", *Journal of Applied Physics*, USA, Vol.85, No.8, April 1999, pp 4403-4405

[4] Guo, Y.G., Zhu, J.G, Watterson, P.A., and Wu, W., "Design and Analysis of a Transverse Flux Machine with Soft Magnetic Composite Core", *The 6th International Conference on Electrical Machines and Systems*, Beijing, China, August 2003

[5] Zhu, J.G and Ramsden, V.S., "Improved Formulations for Rotating Core Losses in Rotating Electrical Machines", *IEEE Transactions on Magnetics*, Vol. 34, 1998, pp 2234-2242

[6] Guo, Y.G., Zhu, J.G., Zhong, J.J., Watterson, P.A., and Wu, W., "An Improved Method for Predicting Iron Losses in SMC Electrical Machines", Proceeding of *International Symposium on Applied Electromagnetics and Mechanics*, Versailles, France, 12 -14 May 2003, pp 78-79

[7] Carter, G.W., "The Electromagnetic Field in Its Engineering Aspects", 2nd Edition, Longmans, London, 1967, pp 243-247